Damage scenario-based approach and retrofitting strategies for seismic risk mitigation: an application to the historical Centre of Sant'Antimo (Italy)

Nicola Chieffo, Antonio Formisano & Tiago Miguel Ferreira

Published online: 01 Apr 2019.

Submit your article to this journal ⬀

View Crossmark data ⬀

Check for updates

Damage scenario-based approach and retrofitting strategies for seismic risk mitigation: an application to the historical Centre of Sant'Antimo (Italy)

Nicola Chieffo[a] (iD), Antonio Formisano[b] (iD) and Tiago Miguel Ferreira[c]

[a]Department of Civil Engineering, Politehnica University of Timişoara, Timisoara, Romania; [b]Dept. of Structures for Engineering and Architecture, University of Naples "Federico II", Naples, Italy; [c]ISISE, Institute of Science and Innovation for Bio-Sustainability (IB-S), Department of Civil Engineering, University of Minho, Portugal

ABSTRACT

In this framework, the current research work aims to analyse a sub-urban sector of the historic centre of Sant'Antimo, located in the province of Naples (Italy), in order to assess the seismic vulnerability of old masonry buildings in this sector and the expected damage scenarios resulting from seismic events with different characteristics. Moreover, in order to mitigate the identified risk, a set of retrofitting techniques are considered and analysed taking into account their contribution for the reduction of the seismic vulnerability of buildings. The vulnerability analysis is performed through the application of an index-based seismic vulnerability assessment approach integrated into a GIS tool in order to identify the structural units (S.U.) most susceptible at damage. Subsequently, typological vulnerability curves, according to the EMS-98 scale, are obtained for the building stock analysed. Finally, a parametric analysis, varying magnitude and seismogenic site-source distance, is performed to obtain and discuss urban damage and loss estimation scenarios in terms of number of collapsed and unusable buildings, as well as number of human casualties, severe injuries and homelessness.

1. Introduction

The large-scale seismic risk is a useful tool for assessing the susceptibility of a sample of buildings to overcome, in a given period of time, a certain seismic event of an assigned intensity. Seismic risk can be understood as the combination of three factors, namely Exposure (E), Vulnerability (V) and Hazard (H). Exposure is connected to the nature, quantity and value of properties and activities of the area that can be influenced directly or indirectly by the seismic event. Vulnerability can be defined as the intrinsic potential of buildings to suffer a certain level of damage when subjected to a seismic event of defined intensity. Finally, the Hazard can be defined as the expected ground motion in a specific site with a certain probability to be exceeded in a given time interval. More precisely, it represents the probability that a certain value of shaking occurs in a given time interval (Cacace, Zuccaro, De Gregorio, & Perelli, 2018; Dolce & Goretti, 2015; McGuire, 1995). In addition, the heterogeneity of buildings, especially in historical centres, is still one of the most important issues concerning the large-scale seismic risk

---

evaluation. However, the risk, independently from the natural phenomena, is to be considered as the attainment of a level of social and economic "losses" (Udías, 2003). It is important to know the urban heterogeneity and the global socio-economic level, to ensure the development of policies and programs that prevent and, therefore, reduce the urban vulnerability in relation to the number of inhabitants and their exposure to natural phenomena. In fact, an important aspect of evaluating the seismic vulnerability of existing buildings is the progressive damage (cyclic fatigue) produced by the seismic impact (Clementi, Gazzani, Poiani, & Lenci, 2016). In some cases, a specific seismic event is characterised by a mainshock with high intensity followed by several aftershocks. Even in the cases where the intensity of the mainshock does not produce any serious damage to the structure (Krstevska et al., 2010), the subsequent seismic event can cause heavy levels of damage and, in some extreme cases, its collapse (Clementi, Quagliarini, Monni, Giordano, & Lenci, 2017; Pierdicca et al., 2016) and for evaluation of economic and social losses, would not only be able to estimate future potential losses due to the occurrence of earthquakes that can affect a particular region, but it should also be used to prepare and implement risk mitigation measures (Calvi & Pinho, 2006). The methodologies used for large-scale estimations are mainly based on observational methodologies for a significant sample of buildings considered as isolate (Benedetti, Benzoni, & Parisi, 1988; Maio, Ferreira, Vicente, & Estêvão, 2016), therefore neglecting the aggregate configuration. This kind of approach was first proposed by the Italian National Group for the Defence against Earthquakes (GNDT), which took profit of post-earthquake damage observations of masonry buildings in Italy (National Group for Protection from earthquake GNDT, 1993). Subsequently, quick methods were proposed by many researchers in several case studies, for instance in Spain (Lantada et al., 2010), Italy (Brando, De Matteis, and Spacone, 2017a; D'Ayala & Paganoni, 2011; Formisano, 2017a), Romania (Armaş, 2012), Portugal (Ferreira, Vicente, Mendes da Silva, Varum, & Costa, 2013, Ferreira, Maio, & Vicente, 2017b; Vicente, Parodi, Lagomarsino, Varum, & Silva, 2011), Nepal (Brando et al., 2017b) and Iran (Azizi-Bondarabadi, Mendes, Lourenço, & Sadeghi, 2016). In addition, some other studies for the urban seismic vulnerability assessment, including estimation of social costs and human losses, were also delivered (Ferreira, Maio, & Vicente, 2017a; Uva, Sanjust, Casolo, & Mezzina, 2016). Among other advantages, these methodologies can be combined with the macroseismic method (Lagomarsino & Giovinazzi, 2006) for the evaluation of damage scenarios. In fact, instead of refined numerical analyses and simplified theoretical approaches (Formisano & Marzo, 2017), the macroseismic methodology allows to evaluate the propensity at damage of a sample of buildings under seismic events defined according to the EMS-98 macroseismic intensity scale (Grünthal, 1998). The characterisation of seismogenic sources in terms of maximum expected magnitude and cyclicity of events (number of "E" events in a "T" period) allowed to define more accurate and realistic seismic scenarios for earthquake mitigation (Cornell, 1968).

The possibility of identifying the most vulnerable buildings in an urban context based on these scenarios makes it possible to limit the effects of seismic phenomena, safeguarding the historical heritage and life of people. The seismic risk analysis on a regional scale requires the development of simplified methods and models capable of characterising both the capacity of buildings exposed to risk and the seismic demand (see, for instance, Iervolino et al., 2007). Therefore, a large-scale risk analysis does not refer to individual structures, but to classes of buildings having vulnerability expressed as a function of structural parameters collected by standard in situ investigations (Quagliarini, Maracchini, & Clementi, 2017).

In this work, different seismic scenarios obtained on the basis of a parametric approach are used to evaluate the seismic risk of an urban sector located in the municipality of Sant'Antimo, a district of Naples (Italy). Such scenarios are subsequently used to estimate different types of losses, from the building uninhabitable condition and collapse to human casualties and homeless, and to analyse the global impact resulting from the adoption of a set of seismic retrofitting techniques. In order to improve the interpretation of the results, they are mapped using the free and open-source GIS software, QGIS (QGIS Development Team, 2014), wherein geo-referenced

Figure 1. The city of Sant'Antimo in the Campania region of Italy.

graphical information are combined and connected to a relational database containing the main structural characteristics of the assessed buildings.

2. Seismic vulnerability assessment of the historical Centre of Sant'Antimo

2.1. Historical news

The municipality of Sant'Antimo (Figure 1) territorially belongs to the Ancient Atella, extended district between the province of Naples and Caserta. The first urban nucleus of Sant'Antimo dates back from IV – III centuries BC. Subsequently to the regular layout of the cadastral division, outlined in the V century BC, it was developed the road scheme of the medieval period, with the characteristic winding roads crossing the building agglomerations erected around the castle and the church.

The city has presently 33,905 inhabitants and sited 16 km far from the historical city of Naples, one of the major and most important urban centres of Southern Italy and one of the most densely populated areas in Europe (Peroni & Tucci, 2010). Over the recent decades, the urban development of this area has been very heterogeneous, conserving a typological majority of historic masonry structures built in the early 1900s and post-World War II. This sector is the centre of the commercial activities of the city, in addition to containing numerous buildings of historical value, such as the Renaissance baronial castle with a first structure dating back to the Middle Ages, the church of Santo Spirito and the chapel of Sant'Antimo priest and martyr.

2.2. Characterisation of the study area

The vulnerability assessment of the sub-sector selected within the historical centre of Sant'Antimo is considered as the initial stage of a wider study having the final purpose to

Figure 2. Top view of the sub-sector selected as a case study (coloured area).

evaluate the seismic risk of the whole urban built-up area. The sub-sector under study, high-lighted in Figure 2, is composed of 42 buildings erected in aggregate. The prevailing construction type is a masonry structure made of tuff block stones, which represent the local masonry obtained by stones extracted from the ground.

The masonry walls present a two-leaf section about 65 cm thick with a poor infill composed of rubble material (*sacco* masonry). The foundations consist of shallow wall footing, which, in practice, consists on arranging the masonry walls directly on the ground at a depth of about 1,50 m. This area is characterised by the presence of cavities with depths of more than 30 m. As for the roofing systems, most of them still retain the traditional construction typology with timber structural elements and steel ties. Albeit in small numbers, reinforced concrete structures were also observed, corresponding to recent interventions carried out from 2000 to 2017, often as a result of the demolition of old buildings and the re-construction of new ones.

In volumetric terms, buildings develop in elevation from 2 to 3 stories. The inter-storey height is about 3,00 to 4,00 m for the first level and 3,00 to 3,50 m for the upper floors. Horizontal structures are generally made of steel-hollow tile floors or timber. However, as often happens, renovations and redistribution of the interior spaces are carried out without careful planning of the interventions that alter the statics of the building. The presence of these vulnerability factors increases the possibility of collapse and instability of such historical buildings when subjected to seismic actions. The lack of connections among perimeter walls orthogonal to each other (corners) does not guarantee a global behaviour of the structure.

In order to perform the vulnerability assessment, and according to the Building Typology Matrix (BTM) (Lagomarsino & Giovinazzi, 2006), the 42 buildings that compose the sub-sector under study were classified into two different typological classes: class M3.3 for the masonry structures with steel floors and a reinforced concrete slab at the roof level (in 36% of the cases); and class and M3.4 for the masonry structures with reinforced concrete floors and roof (64%). Their distribution over the study is presented in Figure 3.
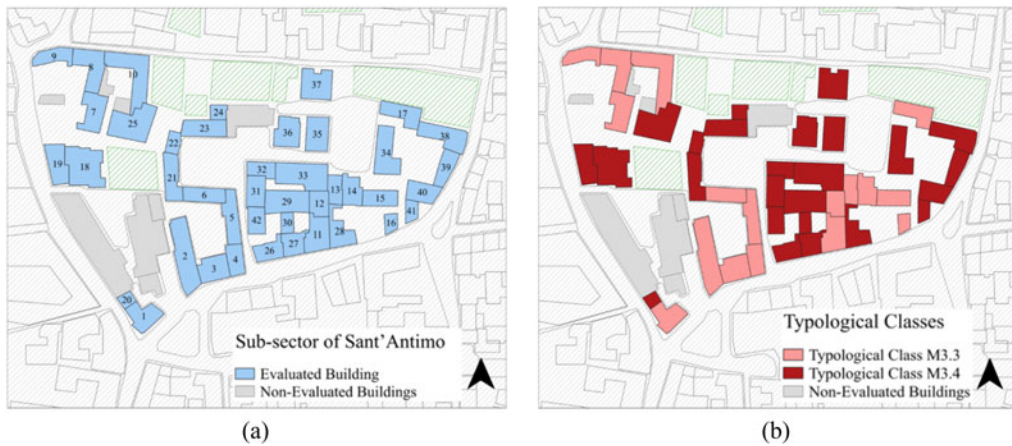
Figure 3. Numbering (a) and typological classes of the masonry buildings (b) in the sub-sector of Sant'Antimo under study.

Table 1. The new vulnerability assessment form for buildings in aggregate.

Parameters	Class Score, S_i				Weight, W_i
	A	B	C	D	
1. Organisation of vertical structures	0	5	20	45	1,00
2. Nature of vertical structures	0	5	25	45	0,25
3. Location of the building and type of foundation	0	5	25	45	0,75
4. Distribution of plan resisting elements	0	5	25	45	1,50
5. In-plane regularity	0	5	25	45	0,50
6. Vertical regularity	0	5	25	45	0,50
7. Type of floor	0	5	15	45	0,80
8. Roofing	0	15	25	45	0,75
9. Details	0	0	25	45	0,25
10. Physical conditions	0	5	25	45	1,00
11. Presence of adjacent building with different height	−20	0	15	45	1,00
12. Position of the building in the aggregate	−45	−25	−15	0	1,50
13. Number of staggered floors	0	15	25	45	0,50
14. Structural or typological heterogeneity among adjacent S.U.	−15	−10	0	45	1,20
15. Percentage difference of opening areas among adjacent facades	−20	0	25	45	1,00

2.3. Seismic vulnerability assessment

Aiming at implementing a quick seismic evaluation procedure for masonry aggregates, it has been used the new vulnerability form proposed in Table 1 (Formisano, Florio, Landolfo, & Mazzolani, 2015, 2017, 2017a; Maio et al., 2015). This new form is based on the Benedetti and Petrini's vulnerability index method (Benedetti & Petrini, 1984), widely used in the past as a rapid technique based on the collection of some features of individual buildings to investigate their vulnerability in case of earthquake. This vulnerability assessment form, composed by 10 basic parameters, was used to recognise the main structural system and the fundamental seismic deficiencies of isolated buildings, as shown in Table 1.

It was adopted with some minor adjustments by the National Group Against Earthquakes as the first screening tool for vulnerability assessment of masonry and RC buildings belonging to historic centres affected by seismic actions. In order to consider the structural interaction between adjacent buildings, not considered in the cited method, a new form was adopted. The new investigation form appropriately conceived for aggregates of masonry buildings is achieved by adding new five parameters to the ten basic parameters of the original form. These new parameters take into account the interaction effects among the aggregated structural units under earthquake (Formisano, Chieffo, & Mosoarca, 2017b; Formisano et al., 2016).
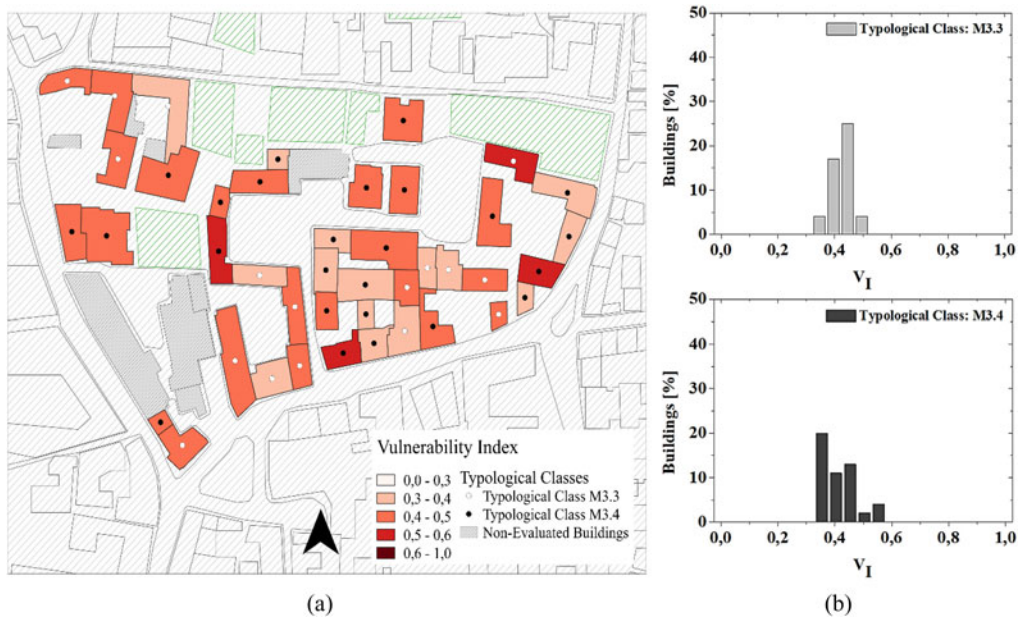
Figure 4. Vulnerability index results: (a) mapping; and (b) histograms for each typological class.

The added parameters, partially derived from previous studies found in literature (Dolce & Goretti, 2015), are:

(1) Parameter 11: Presence of adjacent buildings with different height

The elevation interaction among adjacent buildings takes into account the different height of the adjacent buildings. S.U. located between buildings of the same height or higher are generally the least vulnerable constructions. In fact, the external constructions provide confinement actions on the walls of the building considered when they deform under seismic actions. On the contrary, the most unfavourable cases are when S.U. are located between two lower buildings (one and two floors). In these cases, since the binding action of the adjacent buildings is only partial, the central building is free to deform laterally to the last levels with the possibility of triggering out-of-plane mechanisms.

(2) Parameter 12: Position of the building in the aggregate

This parameter aims to take into account the in-plane interaction among S.U. In particular, this parameter allows to distinguish different positions and, consequently, different structural behaviours of S.U. in the aggregate. Four possible positions are considered: isolated, enclosed between buildings, in corner position and in heading position.

(3) Parameter 13: Number of staggered floors

The presence of staggered floors is contemplated accounting for the effect of pounding caused by floors placed at different heights in adjacent buildings.

(4) Parameter 14: Structural or typological heterogeneity among adjacent S.U.

This parameter accounts for the structural or typological heterogeneity among adjacent S.U. According to the formulation adopted, the building aggregates can be considered homogeneous (from the typological and structural point of view) when they present the same material and the same construction technique, which is the most favourable case. The following situations are also considered: a S.U. adjacent to one made of the same material, but built resorting to a weaker construction technique; a S.U. adjacent to one made of the same material, but built with a better construction technique; a S.U. that has a structural typology very different from the adjacent one (for example a S.U. adjacent to a RC structure).

(5) Parameter 15: Percentage difference of opening areas among adjacent facades
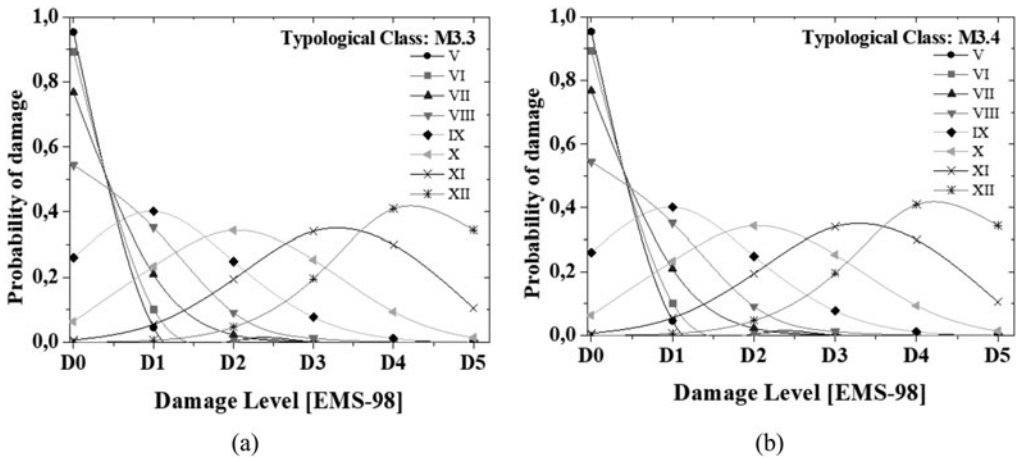
Figure 5. Damage probability matrices for typological classes (a) M3.3 and (b) M3.4.

This parameter takes into account the percentage difference of the opening areas among adjacent S.U.

This factor was evaluated from the premise that percentage of openings influences negatively the seismic response of the façade. Actually, the larger the percentage of openings difference between two adjacent facades, the worse the distribution of horizontal loads between them.

Conceptually, the methodology is based on the calculation of a vulnerability index, I_v, for each S.U. as the weighted sum of the 15 parameters mentioned above. As can be seen in Table 1, these parameters are distributed into four classes (A, B, C and D) with scores S_i of growing vulnerability. Each parameter is characterised by a weight W_i, that can range from 0,25 for the less important parameters to a maximum of 1,50 for the most important ones. According to this, the vulnerability index, I_v, can be calculated according to the following equation:

$$I_V = \sum_{i=1}^{15} S_i \times W_i \tag{1}$$

To facilitate its use and interpretation, the vulnerability index value is normalised in the range $[0 \div 1]$ by means of Equation (2), adopting, from that moment on, the notation V_I.

$$V_I = \left[\frac{I_V - \left(\sum_{i=1}^{15} S_{min} \times W_i \right)}{\left| \sum_{i=1}^{15} \left[(S_{max} \times W_i) - (S_{min} \times W_i) \right] \right|} \right] \tag{2}$$

As illustrated in Figure 4, the application of this procedure to the selected sub-urban sector has allowed to evaluate the seismic vulnerability of the masonry buildings included within it.

From the application of the vulnerability index methodology, it can be seen that the distribution of the vulnerability results is quite homogeneous with an average value of 0,43 for both the typological classes analysed (see Figure 4). The standard deviation (σ_i) associated with the vulnerability index distributions for the analysed typological classes M3.3 and M3.4 is, respectively, $\sigma_{M3.3} = 0,048$ and $\sigma_{M3.4} = 0,062$. The synthetic representation of the statistical data takes place considering the distribution of the frequencies of the vulnerability indices, presented in Figure 4(b). It can be noted that 25% of buildings belonging to the typological class M3.3 have a vulnerability index of 0,45 and only 8% have an index of 0,35. Similarly, for the class M3.4, 20% of buildings have a vulnerability index of 0,35, while 4% of them are associated to a vulnerability index of 0,55.
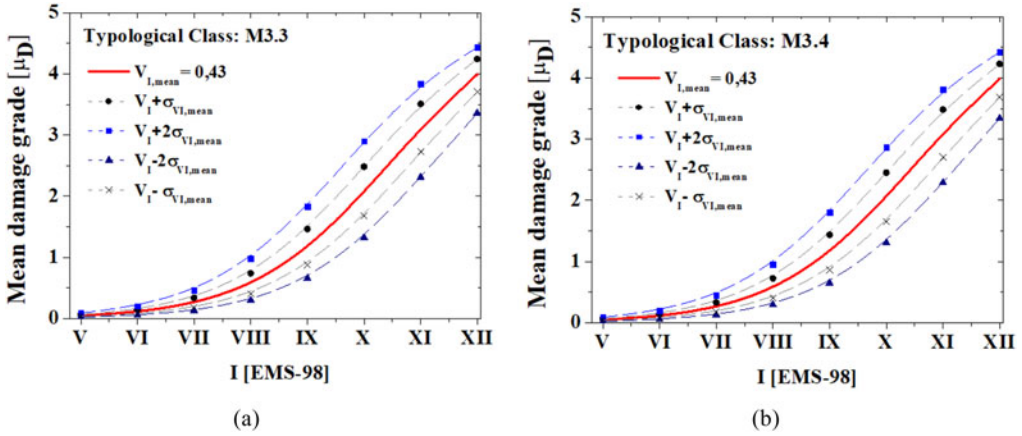
Figure 6. Mean vulnerability curves for building sample of typological classes (a) M3.3 and (b) M3.4.

2.4. Damage distribution: damage probability matrices (DPM) and vulnerability curves

The DPM express the probability of occurrence of a certain level of damage of different typological classes for different levels of seismic intensity according to the EMS-98 scale (Grünthal, 1998).

Methodologically, they can be generated by referring to a scale of generic damage expressed in terms of costs (such as the ratio of the repair cost to the reconstruction cost), which can be understood both in phenomenological terms and according to a qualitative estimate of the different degree of damage that buildings may suffer in case of seismic events.

The proposal of GNDT SSN-2002 working group (Zuccaro & Papa, 1997), whose binomial coefficients are obtained from statistical analysis of the damage suffered by the various building types on the basis of occurred earthquakes, is herein adopted to compute the probability distributions. From the practical point of view, the binomial distribution has the great advantage of being defined by a single parameter, the mean damage level μ_D. The binomial density function, p_k, for the damage score, k, is defined in Equation (3) and shown in Figure 5.

$$p_K = \frac{n!}{k! \cdot (5-k)!} \cdot \left(\frac{\mu_D}{5}\right)^K \cdot \left(1 - \frac{\mu_D}{5}\right)^{5-k} \tag{3}$$

Subsequently, vulnerability curves (Lagomarsino & Giovinazzi, 2006) have been derived to estimate the propensity to damage of the analysed structural units varying the seismic intensity. More in detail, these curves can be properly defined as the probability P[SL|I] that a building reaches a certain limit state "LS" at a given intensity "I" defined according to the European Macroseismic Scale (EMS-98). In particular, as mathematically expressed by Equation (4), vulnerability curves depend on three variables: the vulnerability index (V_I), the macroseismic intensity (I) and a ductility factor Q that describes the ductility of a certain typological class (ranging from 1,0 to 4,0). According to (Lagomarsino, 2006), a mean value of 2,3 was herein assumed for the ductility factor Q.

$$\mu_D = 2,5 \cdot \left[1 + \tanh\left(\frac{I + 6,25 \times V_I - 13,1}{Q}\right)\right] \tag{4}$$

Resorting to Equation (2), it is also possible to derive vulnerability curves using the mean value and the upper and lower bound ranges of the vulnerability index distribution for different scenarios ($V_I - \sigma_{VI,Mean}$; $V_I + \sigma_{VI,Mean}$; $V_I + 2\sigma_{VI,Mean}$; $V_I + 2\sigma_{VI,Mean}$). Such a result is presented in Figure 6(a, b), respectively, for typological classes M3.3 and M3.4.
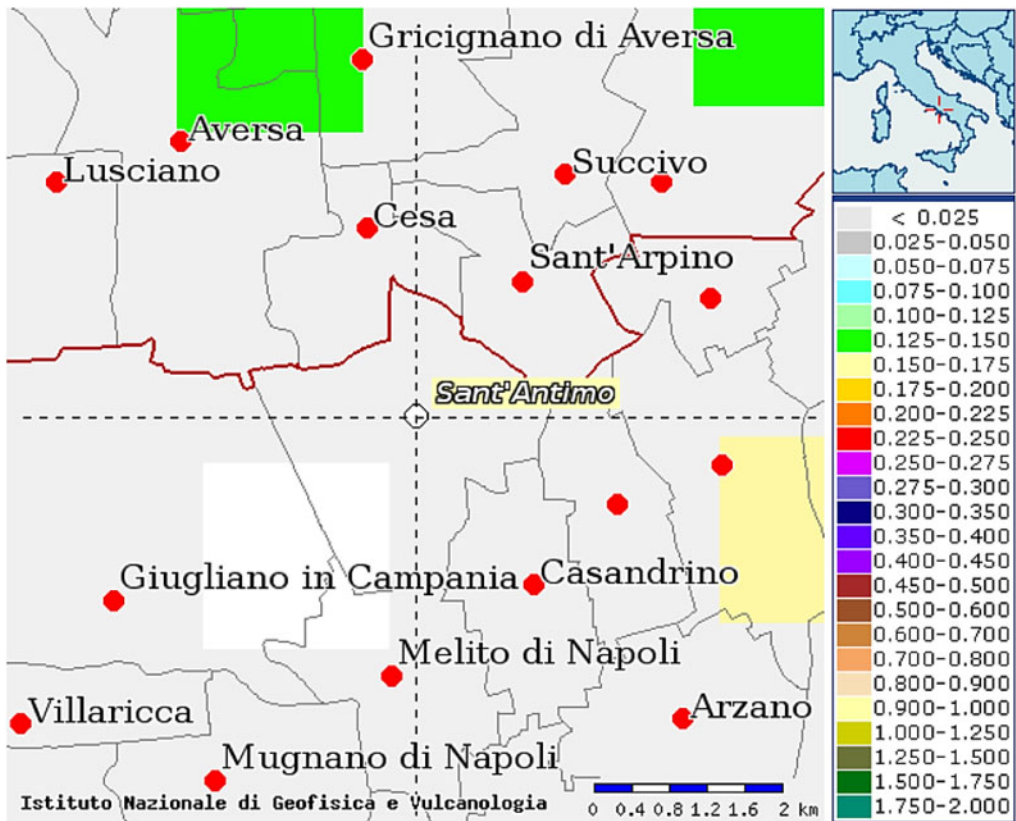
Figure 7. Seismic hazard map of the municipality of Sant'Antimo (DPC-INGV S1).

3. Estimated damage scenarios

3.1. Deterministic damage model prediction

For management and mitigation purposes, risk is usually defined as the economic, social and environmental consequences of a dangerous event that may occur in a given period of time. A prediction on the possible damage scenarios induced by natural events is a useful tool for the quantitative definition of expected losses (Giovinazzi et al., 2004). The proposed study is based on empirical-forecasting analysis, according to which the probable damage scenarios are estimated by means of the disaggregation of the seismic hazard for the *N-sources* combined. Such a procedure is usually obtained by accumulating each moment magnitude, M_w, and site-source distance, R, as well as the contribution to the global hazard, λ. Therefore, disaggregating the hazard in terms of M_w and R has lately become a routine practice in the seismic hazard evaluation community (Barani et al., 2009; Bazzurro & Cornell, 1999).

Formally, therefore, this disaggregation represents the conditional probability distribution of M_w, R, given the event that S_a exceeds a fixed-level intensity (IM_s) at the site. According to the seismic hazard map, proposed by *National Institute of Geophysics and Volcanology*, INGV (National Institute of Geophysics and Vulcanology, n.d.) the city of Sant'Antimo is characterised by a maximum expected PGA of 0,25 g (medium-high seismicity) with a probability of exceeding 10% in 50 years, see Figure 7. Furthermore, based on the disaggregation of the PGA's, the maximum moment magnitude estimated is $M_w = 5,15$. Based on these considerations, a set of moment magnitude, M_w, were selected in the range from 4 to 6.

Table 2. Correlation between moment magnitude, M_w, and macroseismic intensities, I_{EMS-98}, for different seismogenic site-source distances.

Magnitude, M_w	Macroseismic Intensity, I_{EMS-98}		
	$R = 7$ (km)	$R = 21$ (km)	$R = 35$ (km)
4	IX	VI	V
5	XI	VIII	VII
6	XII	IX	VIII

To this purpose, a range of macroseismic magnitude, between $I_{EMS-98} =$ VIII and XII, site-source distances and focal depth between 5 and 25 km, have been considered (Chieffo et al., 2019). Subsequently, the attenuation relationship of seismic effects proposed by Esteva (1974), reported in Equations (5) and (6), is also adopted as follows:

$$I_{EMS-98} = 1,45 \cdot M_w - 2,46 \ln(R) + 8,166 \qquad (5)$$

$$R = \sqrt{d^2 + h^2{}_f} \qquad (6)$$

where M_w is the moment magnitude and R is the site-source distance expressed in kilometres, which, as detailed in Equation (5), depends on the epicentre distance (d_i) and the focal depth (h_f). The correlation obtained between moment magnitude, M_w, and macroseismic intensity, I_{EMS-98}, for different site-source distances is summarized in Table 2.

As one can observe from the analysis of the values presented in Table 2, when the site-source distance increases, the seismic intensity tends to attenuate progressively. Furthermore, referring to the damage parameter μ_D, it is possible to obtain nine damage scenarios, presented in Figure 8.
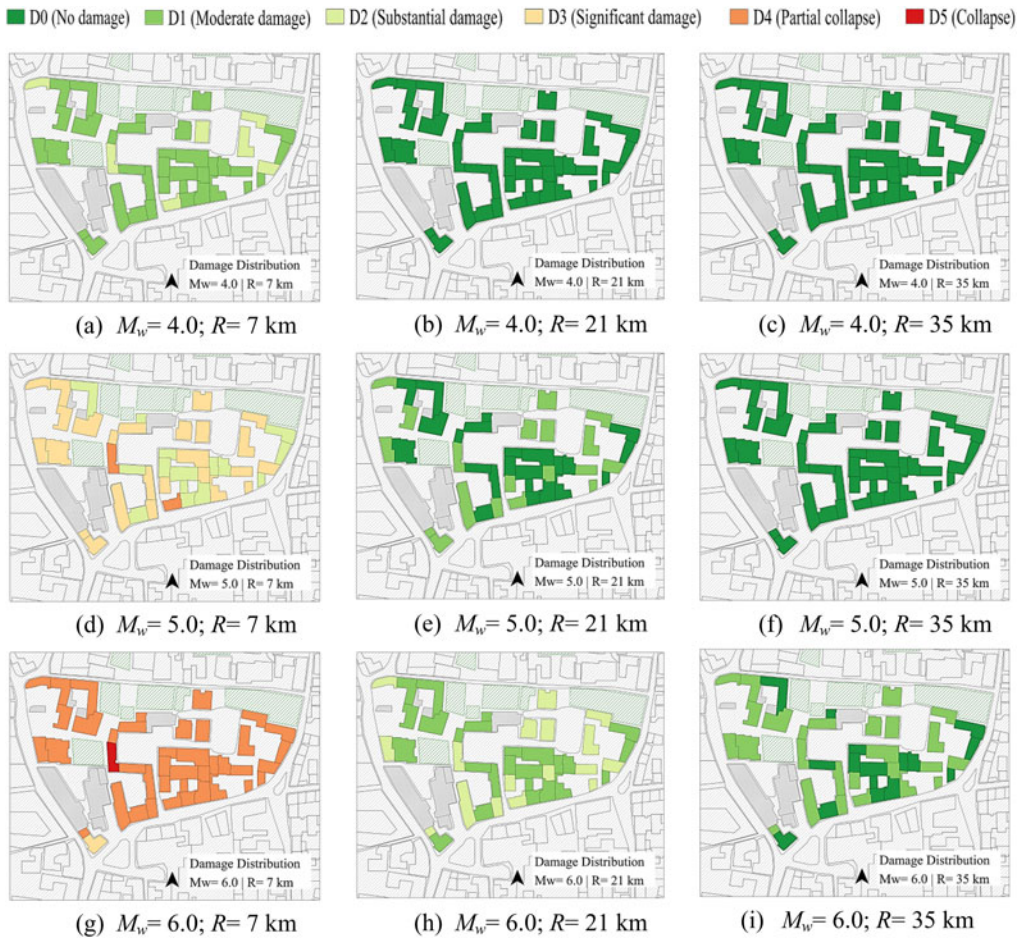
From the previous figure, it is possible to note that, when increasing the site distance, the expected damage tends to decrease because the seismic intensity is greatly attenuated. As an example, for a site-source distance of 7 km and a moment magnitude of 6,0, according the attenuation law proposed by Esteva (1974), it is expectable that most of the buildings reach damage thresholds D4 (partial collapse). Differently, by increasing the distance up to a maximum of 35 km and by leaving unaltered the magnitude, the seismic effects are attenuated and, therefore, damage levels D0 (no damage) and D1 (moderate) are expectable. Figure 9 shows the damage distribution obtained for the above-described combinations. As can be observed in Figure 8, for a moment magnitude M_w equal to 4,0 and a site-source distance of 7 km, it is expected that 83% of the buildings reach damage level D1 and 17% reach damage level D2. For the same moment magnitude, if the distance tends to increase either to 15 km or 30 km, it is expectable that all buildings remain with no damage (D0). However, it can be noted that the most severe combination was found for distance $R = 7$ km with a moment magnitude $M_w = 6$.

3.2. Fragility curves

Considering the average of vulnerability indices associated to a specific class of buildings, it was possible to define the fragility curves for the typological classes. Fragility curves are used to represent the estimated damage and to define the probability of overcoming a certain degree or state of damage, D_k, enclosed in the range [0 ÷ 5]. This probability is obtained directly from the physical damage distributions of the building derived from the *beta* probability function for a given type of buildings. Equation (7) shows the discrete probabilities, $P[D_k = d]$, derived from the cumulative probability difference $P[D_i \geq d]$.

$$P[D_K = d] = P[D_K \geq d] - P[D_{K+1} \geq d] \qquad (7)$$

In this particular case, the analysed vulnerability classes present on average the same vulnerability index, which means that the shape of the fragility curves are exactly the same for both typological classes considered in this study, see Figure 10(a). Moreover, Figure 10(b) shows the

■ D0 (No damage) ■ D1 (Moderate damage) ■ D2 (Substantial damage) ■ D3 (Significant damage) ■ D4 (Partial collapse) ■ D5 (Collapse)

(a) M_w= 4.0; R= 7 km   (b) M_w= 4.0; R= 21 km   (c) M_w= 4.0; R= 35 km

(d) M_w= 5.0; R= 7 km   (e) M_w= 5.0; R= 21 km   (f) M_w= 5.0; R= 35 km

(g) M_w= 6.0; R= 7 km   (h) M_w= 6.0; R= 21 km   (i) M_w= 6.0; R= 35 km

Figure 8. Damage scenarios of the investigated sector within the historical centre of Sant'Antimo.

average damage distributions obtained by means of the binomial distribution by varying the macroseismic intensity (I_{EMS-98}) in the range [V ÷ XII]

4. Retrofitting techniques for risk mitigation

4.1. Description of intervention strategies

The vulnerability of unreinforced masonry buildings (URM) to compromised performance is a serious issue. Such structural types, usually constructed of bricks or blocks and some older cut stone buildings, have been designed primarily to resist gravity loads with little or no consideration for lateral actions (Keller et al., 2017; Clementi et al., 2017).

Although URM buildings function satisfactorily in the presence of service loads, they can be severely damaged in the presence of high lateral loads, such as earthquake inertia forces (Clementi et al., 2018). The demolition and replacement of these old masonry structures is generally not feasible due to the enormous effort and cost of the new construction.

Consequently, for risk mitigation, especially in areas with high population density, retrofit strategies are a solution to reduce the seismic emergency problem. In the specific case, in order to improve the building's behaviour also in a cost-effective perspective, two distinct solutions are taken into consideration: steel tie rods (TR) (Ferreira et al., 2017a) and floor shear connectors
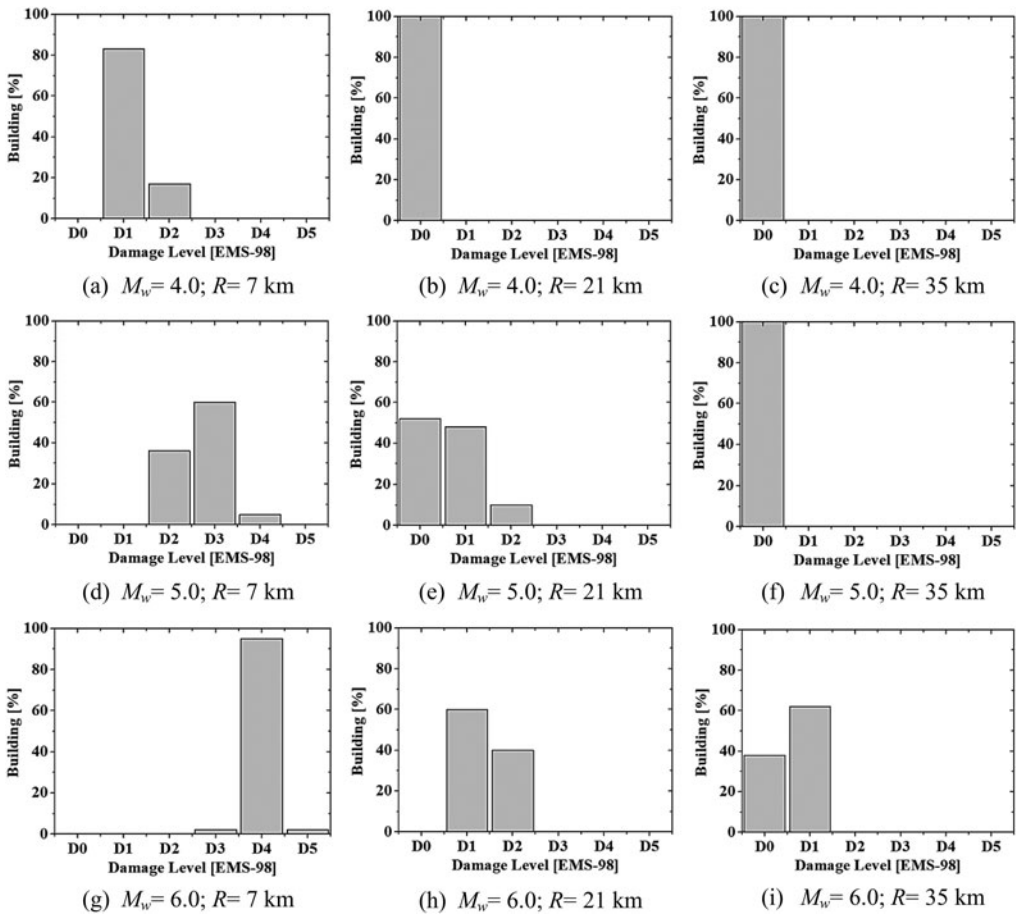
Figure 9. Damage distributions for different epicentre distance and moment magnitude combinations.
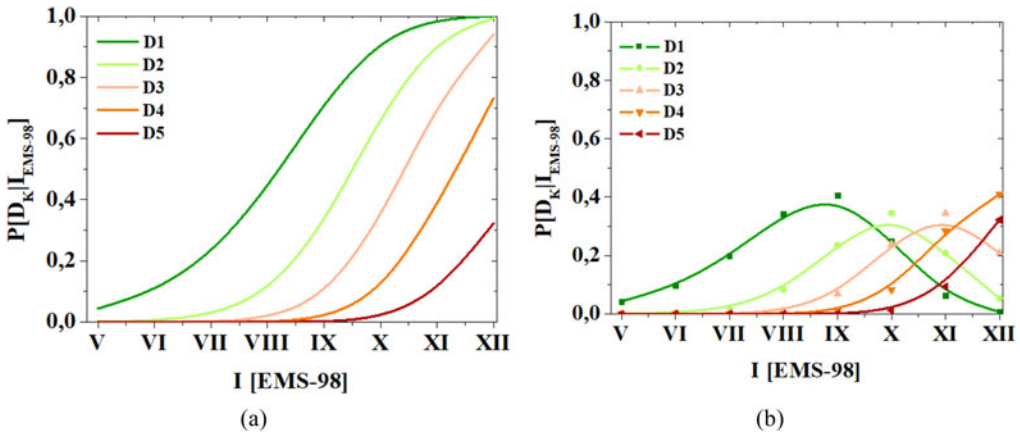
Figure 10. Typological fragility curves (a) and damage distribution functions (b).

(FSC) (Leca, 2015), as reported in Figure 10. Specifically, the TR system guarantees an important constraint between perimeter walls, a prerequisite for the survival of the building to seismic actions. This intervention technique consists in preparing a steel tie rod with a diameter

Steel tie-rod anchorage

Steel tie-rod

Vertical cross section

Steel tie-rod anchorage

Main elevatiton

(a) adapted from (Ferreira et al., 2017a)

60 mm

43 mm

40 mm

37 mm

65 mm

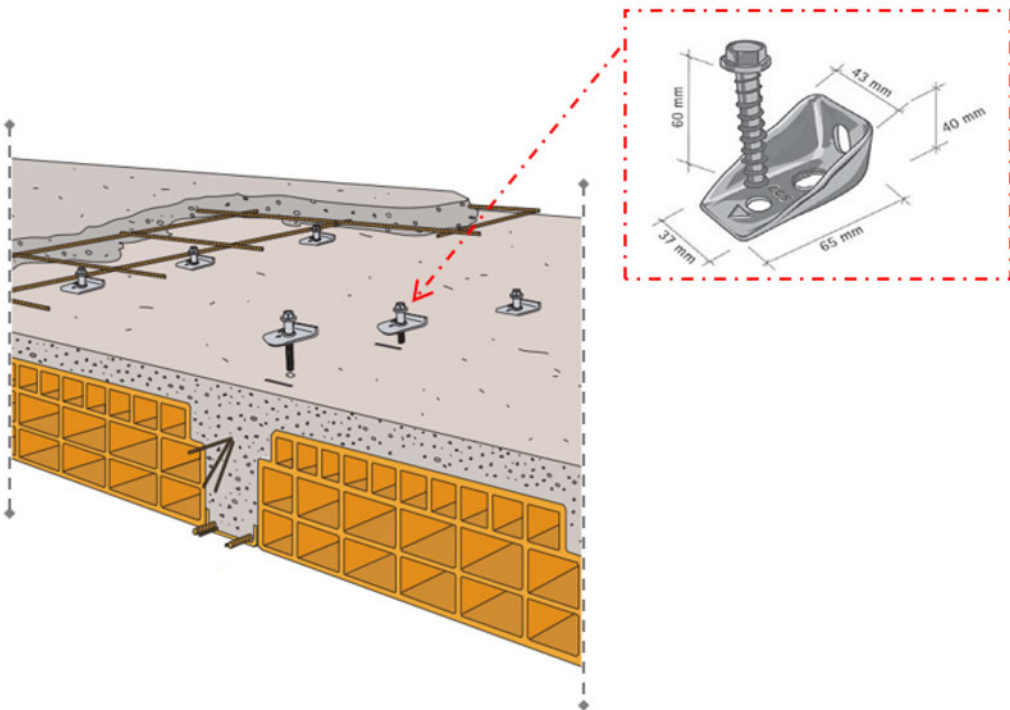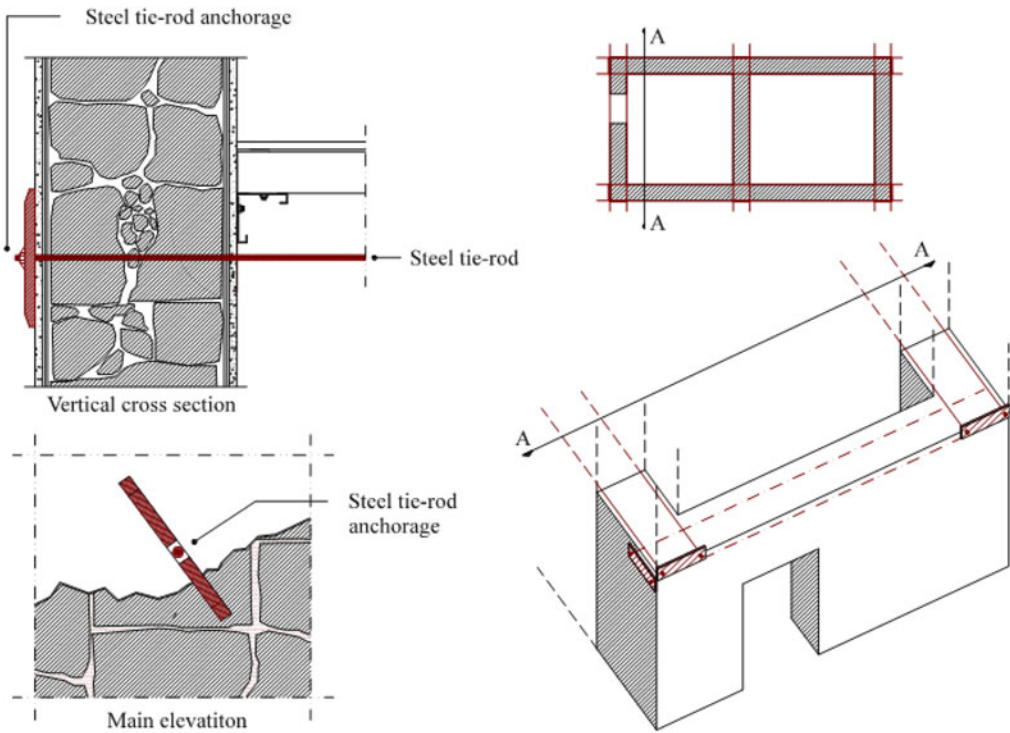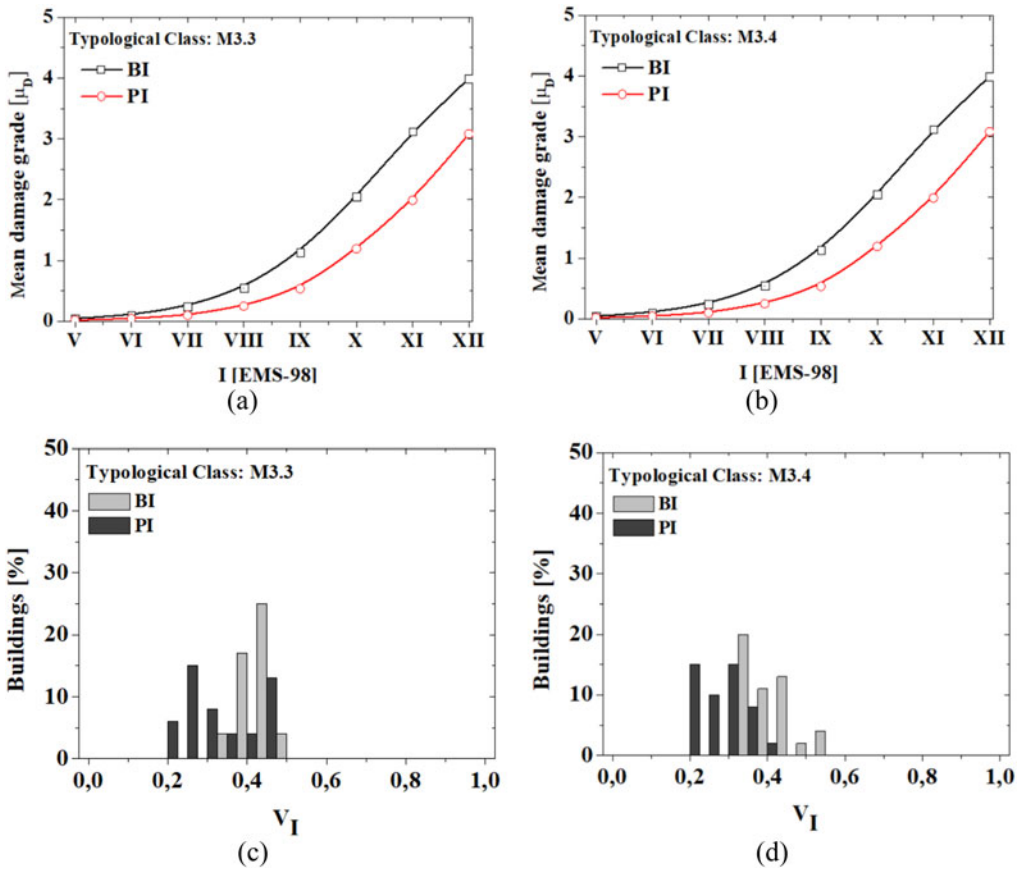(b) adapted from (Leca, 2015)

Figure 11. Retrofitting solutions: (a) steel tie rods (TR) and (b) floor shear connectors (FSC).

Figure 12. Before (BI) and Post (PI) interventions mean vulnerability curves for typological classes (a) M3.3 and (b) M3.4 and vulnerability frequencies distributions for building classes (c) M3.3 and (d) M3.4.

$16 \, \text{mm} \leq \phi \leq 20 \, \text{mm}$, in a horizontal position on both walls and fixed by metal plates in order to guarantee a box behaviour of the structure, Figure 11(a).

In the case of the second technique, illustrated in Figure 11(b), the use of shear connectors and steel grid allows to increase the cooperating concrete slab and therefore the height of the slab's section, avoiding therefore the formation of cracks induced by the flexural regime. In this case, the increase in resistance is proportional to the increase in the height of the section (Ruiz et al., 2010).

4.2. Post intervention and damage scenario distributions

As discussed in Section 4.1, the proposed intervention techniques improve the behaviour of the analysed building sample. The proposed intervention techniques (PI = TR + FSC) will be indistinctly applied to all buildings in the study area. In this case, the box behaviour is guaranteed with the steel tie rods, while, considering the shear connectors and steel grid, in-plane resistance of the existing floors is increased. In methodological terms, this can be done by reassessing the vulnerability classes, S_i, of the parameters that are related to those features, namely of Parameter 1, which evaluates the organisation of the vertical structures, Parameter 7, which evaluates the horizontal diaphragms, and Parameter 8, which evaluates the roofing system. The buildings were thus virtually retrofitted by upgrading the original vulnerability classes of these parameters to class B, in the case of P1 and P7, and A, in the case of P8, resulting in the reduction of their

Table 3. Mean vulnerability distributions related to the cases of before (BI) and post (PI) interventions.

Typological class	BI		PI			
	V_I	σ_i	V_I	σ_i	ΔV_I [%]	$\Delta \sigma_i$ [%]
M3.3	0,43	0,048	0,26	0,046	−39	−4,16
M3.4	0,43	0,062	0,26	0,055	−39	−11,29

vulnerability indexes values, I_v, and, consequently, in the decrease of their mean damage grade values, μ_D.

Figure 12(a,b) present the comparison among the mean vulnerability curves for the typological classes M3.3 and M3.4 before (BI) and after (PI) interventions, respectively. In addition, Figures 12(c,d) show in the same cases the vulnerability distributions for the two inspected building classes.

The characteristic results obtained for the new vulnerability distribution (after intervention) are summarized in Table 3.

From the analysis of results given in Table 3, it is possible to see how the use of the two retrofitting systems herein investigated are able to improve the global behaviour of the building sample. In fact, as can be seen, there is a vulnerability reduction of about 39% for both typological classes. Statistically, the standard deviation provides a measure of the magnitude of the sample variation examined with a reduction of 4,16% and 11,29% for typological classes M3.3 and M3.4, respectively.

Adopting the same presentation scheme followed in Section 3, Figure 13 presents the damage scenarios obtained for the *post* interventions (PI) condition, considering the nine site-source conditions detailed in Table 2.

4.3. Collapsed and unusable buildings

The consequences of seismic events in terms of collapsed and unusable buildings are evaluated in this work following the empirical correlations proposed for the Italian territory in (Bramerini & Lucantoni, 2000) on the basis of the observed damages. Thus, and resorting to Equations (8) and (9), probabilities of collapsed and unusable buildings are estimated for the above-presented damage scenarios, see Figure 13.

$$N_{coll.} = D5 + 0,4 \times D4 \qquad (8)$$

$$N_{unus.} = 0,6 \times (D4 + D3) + 0,6 \times D2 \qquad (9)$$

Regarding the probabilities of building failures, it is possible to perceive that the percentage of collapses tends to decrease proportionally when the distance R increase. The overall results for the different combinations considered are summarised in Table 4.

From the analysis of results, it is worth noting that, with the application of the two retrofitting solutions, there is a reduction of the seismic impact both in terms of collapsed and unusable buildings. Focusing on the worst-case scenario ($R = 7$, $M_w = 6,0$), we moved from a situation where 40% of the buildings are expected to collapse, to a situation without any collapse (see Table 4).

4.4. Human casualties and homelessness

From the analysis of the impacts in terms of collapsed and unusable buildings presented in Section 4.2, it is further possible to estimate casualty rates (number of deaths and severely injured) and homelessness.

As discussed in Zuccaro and Cacace (2015), such rates can be estimated considering that there is a direct consequence between them and the probability of exceeding a damage

■ D0 (No damage) ■ D1 (Moderate damage) □ D2 (Substantial damage) □ D3 (Significant damage) ■ D4 (Partial collapse) ■ D5 (Collapse)

(a) M_w= 4.0; R= 7 km   (b) M_w= 4.0; R= 21 km   (c) M_w= 4.0; R= 35 km

(d) M_w= 5.0; R= 7 km   (e) M_w= 5.0; R= 21 km   (f) M_w= 5.0; R= 35 km

(g) M_w= 6.0; R= 7 km   (h) M_w= 6.0; R= 21 km   (i) M_w= 6.0; R= 35 km
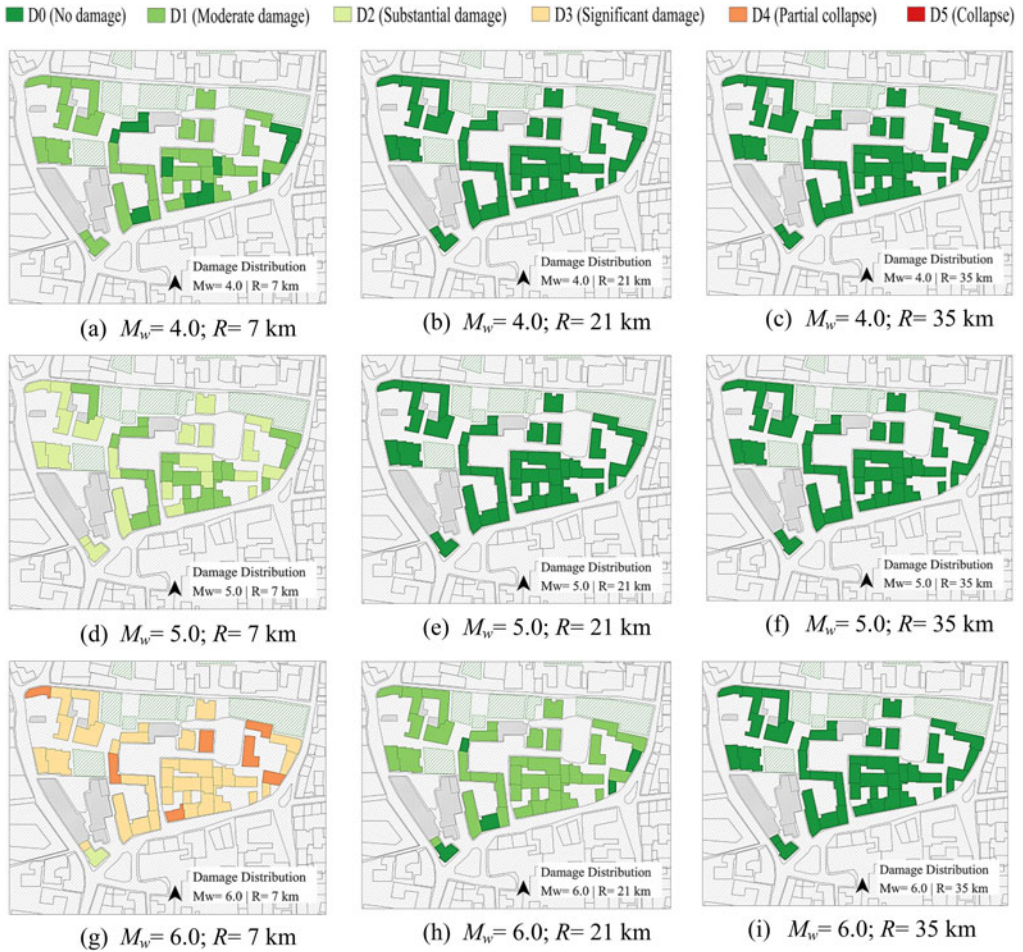
Figure 13. Post intervention (PI) damage scenarios for different magnitudes and site-source distances.

Table 4. Estimation of collapsed and unusable buildings for different combinations of moment magnitude and site-source distance related to the cases of before (BI) and post (PI) interventions.

	Number of collapsed and unusable buildings (BI)					
	$M_w = 4,0$		$M_w = 5,0$		$M_w = 6,0$	
Site-source distance, R (km)	Collapsed	Unusable	Collapsed	Unusable	Collapsed	Unusable
7	–	7 (10%)	2 (2%)	25 (60%)	17 (40%)	24 (57%)
21	–	–	–	–	–	–
35	–	–	–	–	–	–

	Number of collapsed and unusable buildings (PI)					
	$M_w = 4,0$		$M_w = 5,0$		$M_w = 6,0$	
Site-source distance, R [km]	Collapsed	Unusable	Collapsed	Unusable	Collapsed	Unusable
7	–	–	–	14 (34%)	–	25 (60%)
21	–	–	–	–	–	–
35	–	–	–	–	–	–

Table 5. Estimation of human casualties and homelessness for different combinations of moment magnitude and site-source distance related to the cases of before (BI) and post (PI) interventions.

	Number of casualties and homeless people (BI)					
	$M_w = 4,0$		$M_w = 5,0$		$M_w = 6,0$	
Site-source distance, R [km]	Death	Homeless	Death	Homeless	Death	Homeless
7	–	–	3 (2%)	92 (60%)	62 (40%)	87 (57%)
21	–	–	–	–	–	–
35	–	–	–	–	–	–

	Number of casualties and homeless people (PI)					
	$M_w = 4,0$		$M_w = 5,0$		$M_w = 6,0$	
Site-source distance, R [km]	Death	Homeless	Death	Homeless	Death	Homeless
7	–	–	–	52 (34%)	10 (7%)	92 (60%)
21	–	–	–	–	–	–
35	–	–	–	–	–	–

threshold D4 and D5, see Equation (10):

$$N_{m,r} = \frac{N_{Tot,res.}}{N_{bld}} \tag{10}$$

where $N_{m,\,r}$ is the average number of residents in the analysed area, $N_{tot,\,res}$ is the total number of residents (153) and N_{bld} is the total number of buildings investigated (42).

Subsequently, the number of deaths and homelessness is assessed according to the number of collapsed and unusable buildings by using the following Equations (11) and (12):

$$N_{died} = N_{m,r} \times N_{coll.} \tag{11}$$

$$N_{hmls} = N_{m,r} \times N_{unus.} \tag{12}$$

where N_{died} and N_{hmls} are, respectively, the number of dead and homeless, i.e., people living in buildings that it is expected to suffer partial (D4) or total collapse (D5) or in buildings that it is expected to suffered substantial damage (D2), significant damage (D3) or partial collapse (D4), respectively. As mentioned before, $N_{coll.}$ and N_{unus} stand, respectively, for the number of collapsed and unusable buildings. The overall results for each moment magnitude *versus* epicentre distance combination are presented in Table 5.

Similarly, to what was analysed in the previous section, referring to the worst-case scenario, there is a reduction of 33% of the number of casualties, from 62 to 10 injured and/or dead people.

5. Conclusion

The study analysed the seismic vulnerability of an urban sector in the historic centre of Sant'Antimo by using a parametric-probabilistic approach. The city of Sant'Antimo is located in an area characterised by medium to high seismicity with expected PGAs values included in the range [0,15g ÷ 0,25g].

The assessment of seismic vulnerability has been analysed by means of a quick approach, allowing to identify the propensity of buildings to suffer a certain damage grade. The statistical distribution of vulnerability indices shows, globally, a medium to high vulnerability of the area.

This aspect is related to the presence of buildings that show substantial deficiencies. Afterwards, the vulnerability curves have been defined in order to characterise, on average, the expected damage by varying the seismic intensity according to the EMS-98 scale. It is important to note that, for moderate values of seismic intensity ($I_{EMS-98} < X$) the expected damage has not

been relevant, but for high values of seismic intensity (X$<I_{EMS-98}<$ XII), the expected damage would cause an incipient collapse of the analysed sample. Analysis of the damage and loss scenario by means parametric approach have been considered using the attenuation law in terms of seismic intensity proposed by Esteva. Having defined a set of magnitude (M_w) and site-source distances (R), it has been possible to analyse in detail the influence of these factors on an urban-scale and estimate the associated damage caused by different earthquakes. The results obtained have shown that, for distances very close to the site of interest, the expected damage increases with increasing seismic intensity. In fact, for $R = 7$ km and $M_w = 6$, it corresponds to the most severe scenario.

The representation of spatial data has been made by using the GIS tool, an effective integrated support for the mitigation and management of the seismic emergency.

Risk mitigation is an important preparatory aspect for planning and developing possible interventions for reducing the vulnerability and safeguard the people. Two distinct intervention techniques have been applied indiscriminately to the typological classes examined in order to improve their seismic behaviour. In this sense, steel tie rods and shear connectors have been considered for the purpose of increasing the global behaviour of structures studied.

From a critical comparison of the results obtained from the losses point of view, it is worth noting that the adoption of appropriate retrofitting systems reduces the possibility of structural collapse by 40%. However, the uselessness buildings increase of 3%. The seismic scenarios have been mitigated for seismogenic site-source distances of 21 and 35 km, respectively. In this case, the effects induced by the earthquake have not caused any substantial damage. In conclusion, the proposed study implements a parametric procedure, based on macroseismic approach, for the prediction of possible damage scenarios and expected physical impacts in urban areas.

In this sense, this research could be developed in other historical centres, so to become a very useful tool for appropriate risk mitigation plans.

ORCID

Nicola Chieffo 🔾 http://orcid.org/0000-0001-5714-3334
Antonio Formisano 🔾 http://orcid.org/0000-0003-3592-4011

References

Armaş, I. (2012). Multi-criteria vulnerability analysis to earthquake hazard of Bucharest, Romania. *Natural Hazards*, 8(2), 182–195.

Azizi-Bondarabadi, H., Mendes, N., Lourenço, P. B., & Sadeghi, N. H. (2016). Empirical seismic vulnerability analysis for masonry buildings based on school buildings survey in Iran. *Bulletin of Earthquake Engineering*, 14(11), 3195–3229. doi:10.1007/s10518-016-9944-1

Barani, S., Spallarossa, D., & Bazzurro, P. (2009). Disaggregation of probabilistic ground-motion Hazard in Italy. *Bulletin of Seismological Society of America*, 99(5), 2638–2661. doi:10.1785/0120080348

Bazzurro, P., & Cornell, C. A. (1999). Disaggregation of seismic hazard. *Bulletin of Seismological Society of America*, 89, 501–520.

Benedetti, D., Benzoni, G., & Parisi, M. A. (1988). Seismic vulnerability and risk evaluation for old urban nuclei. *Earthquake Engineering & Structural Dynamics*, 16, 183–201. doi:10.1002/eqe.4290160203

Benedetti, D., & Petrini, V. (1984). Sulla vulnerabilità si sismica di edifici in muratura: Un metodo di valutazione. *L'Industria Delle Costruzioni*, 18, 66–74.

Bramerini, F., & Lucantoni, A. (2000). Analysis of different earthquake damage scenarios for emergency planning in Italy. *In Management Information Systems*, 45, 1–10.

Brando, G., De Matteis, G., & Spacone, E. (2017). Predictive model for the seismic vulnerability assessment of small historic centres: Application to the inner Abruzzi Region in Italy. *Engineering Structure*, 153, 81–96. doi:10.1016/j.engstruct.2017.10.013

Brando, G., Rapone, D., Spacone, E., O'Banion, M. S., Olsen, M. J., Barbosa, A. R., … Stravidis, A. (2017). Damage Reconnaissance of Unreinforced Masonry Bearing Wall Buildings After the 2015 Gorkha, Nepal, Earthquake. *Earthquake Spectra*, 33(S1), s243–s273. doi:10.1193/010817EQS009M

Cacace, F., Zuccaro, G., De Gregorio, D., & Perelli, F. L. (2018). Building Inventory at National scale by evaluation of seismic vulnerability classes distribution based on Census data analysis: BINC procedure. *International Journal Disaster Risk Reduction*, 28, 384–393. doi:10.1016/j.ijdrr.2018.03.016

Calvi, G., & Pinho, R. (2006). Development of seismic vulnerability assessment methodologies over the past 30 years. *ISET. Journal of Earthquake Technology*, 43, 75–104.

Chieffo, N., Mosoarca, M., Formisano, A., & Apostol, I. (2019). *Seismic vulnerability assessment and loss estimation of an urban district of Timisoara*. IOP Conference Series: Materials Science and Engineering, 2018; Vol. 471, ISSN: 1757-899X

Clementi, F., Gazzani, V., Poiani, M., & Lenci, S. (2016). Assessment of seismic behavior of heritage masonry buildings using numerical modeling. *Journal of Building Engineering*, 8, 29–47. doi:10.1016/j.jobe.2016.09.005

Clementi, F., Gazzani, V., Poiani, M., Mezzapelle, P. A., & Lenci, S. (2018). Seismic assessment of a monumental building through nonlinear analyses of a 3D solid model. *Journal of Earthquake Engineering*, 22(sup1), 35–61. doi:10.1080/13632469.2017.1297268

Clementi, F., Quagliarini, E., Monni, F., Giordano, E., & Lenci, S. (2017). Cultural heritage and earthquake: The case study of "Santa Maria della Carità" in Ascoli Piceno. *The Open Civil Engineering Journal*, 11(Suppl 5, M5), 1079–11058. doi:10.2174/1874149501711011079

Clementi, F., Pierdicca, A., Formisano, A., Catinari, F., & Lenci, S. (2017). Numerical model upgrading of a historical masonry building damaged during the 2016 Italian earthquakes: The case study of the Podestà palace in Montelupo (Italy). *Journal of Civil Structural Health Monitoring*, 7(5), 703–717. doi:10.1007/s13349-017-0253-4

Cornell, C. A. (1968). Engineering seismic risk analysis. *Bulletin of Seismological Society of America*, 58(5), 1583–1606.

D'Ayala, D. F., & Paganoni, S. (2011). Assessment and analysis of damage in L'Aquila historic city centre after 6th April 2009. *Bulletin of Earthquake Engineering*, 9, 81–104. doi:10.1007/s10518-010-9224-4

Dolce, M., & Goretti, A. (2015). Building damage assessment after the 2009 Abruzzi earthquake. *Bulletin of Earthquake Engineering*, 13(8), 2241–2261. doi:10.1007/s10518-015-9723-4

Esteva, L. (1974). *Geology and probability in the assessment of seismic risk*. Paper presented at the 2nd International Conference of the Association of Engineering Geology, Sao Paulo.

Ferreira, T. M., Maio, R., & Vicente, R. (2017a). Analysis of the impact of large scale seismic retrofitting strategies through the application of a vulnerability-based approach on traditional masonry buildings. *Earthquake Engineering and Engineering Vibration*, 16(2), 329–348. doi:10.1007/s11803-017-0385-x

Ferreira, T. M., Maio, R., & Vicente, R. (2017b). Seismic vulnerability assessment of the old city centre of Horta, Azores: calibration and application of a seismic vulnerability index method. *Bulletin of Earthquake Engineering*, 15(7), 2879–2899. doi:10.1007/s10518-016-0071-9

Ferreira, T. M., Vicente, R., Mendes da Silva, J. A. R., Varum, H., & Costa, A. (2013). Seismic vulnerability assessment of historical urban centres: case study of the old city centre in Seixal, Portugal. *Bulletin of Earthquake Engineering*, 11(5), 1753–1773. doi:10.1007/s10518-013-9447-2

Formisano, A. (2017a). Local- and global-scale seismic analyses of historical masonry compounds in San Pio delle Camere (L'Aquila, Italy). *Natural Hazards*, 86(S2), 465–487. doi:10.1007/s11069-016-2694-1

Formisano, A. (2017b). Theoretical and numerical seismic analysis of masonry building aggregates: Case studies in San Pio Delle Camere (L'Aquila, Italy). *Journal of Earthquake Engineering*, 21(2), 227–245. doi:10.1080/13632469.2016.1172376

Formisano, A., Chieffo, N., & Fabbrocino, F. (2016, December). *The influence of local mechanisms on large scale vulnerability estimation of masonry building aggregates*. In AIP Conference Proceedings. Proceeding of 14th International Conference of numerical analysis and applied mathematics (pp. 1–6). Rhodes, Greece.

Formisano, A., Chieffo, N., Fabbrocino, F., & Landolfo, R. (2017, July). *Seismic vulnerability and damage of Italian historical centre: a case study in the Campania region*. In AIP Conference Proceedings. Proceeding of 14th International Conference of numerical analysis and applied mathematics (pp. 1–6). Rhodes, Greece.

Formisano, A., Chieffo, N., & Mosoarca, M. (2017b). Seismic vulnerability and damage speedy estimation of an urban sector within the Municipality of San Potito Sannitico (Caserta, Italy). *The Open Civil Engineering Journal*, 12, 1106–1121. doi:10.2174/1874149501711011106

Formisano, A., Florio, G., Landolfo, R., & Mazzolani, F. M. (2015). Numerical calibration of an easy method for seismic behaviour assessment on large scale of masonry building aggregates. *Advances in Engineering Software*, 80, 116–138. doi:10.1016/j.advengsoft.2014.09.013

Formisano, A., & Marzo, A. (2017). Simplified and refined methods for seismic vulnerability assessment and retrofitting of an Italian cultural heritage masonry building. *Computers and Structures*, 180, 13–26. doi:10.1016/j.compstruc.2016.07.005

Giovinazzi, S., Balbi, A., & Lagomarsino, S. (2004, January). *Un modello di vulnerabilità per gli edifici nei centri storici*. Proceeding of XI ANIDIS Congresso Nazionale ANIDIS, L'Ingegneria Sismica in italiana, Genova, Italy.

Grünthal, G. (1998). European Macroseismic Scale 1998. In Grünthal, G (Ed.), *Chaiers du Centre Européen de Géodynamique et de Séismologie*, Vol. 15. Luxembourg: European Center for Geodynamics and Seismology, ISBN 2879770084.

Iervolino, I., Giorgio, M., & Manfredi, G. (2007). Expected loss-based alarm threshold set for earthquake early warning systems. *Earthquake Engineering & Structural Dynamics*, 36, 1151–1168. doi:10.1002/eqe.675

Keller, A., Chieffo, N., Opritescu, E., Mosoarca, M., & Formisano, A. (2017). Resilience of Historic Cities and Adaptation To Climate Change. *Urban Architecture & Construction*, 8, 15–26.

Krstevska, L., Tashkov, L., Naumovski, N., Florio, G., Formisano, A., Fornaro, A., & Landolfo, R. (2010). *In-situ experimental testing of four historical buildings damaged during the 2009 L'Aquila earthquake*. COST ACTION C26: Urban Habitat Constructions under Catastrophic Events – Proceedings of the Final Conference, 427–432.

Lagomarsino, S. (2006). On the vulnerability assessment of monumental buildings. *Bulletin of Earthquake Engineering*, 4(4), 445–463. doi:10.1007/s10518-006-9025-y

Lagomarsino, S., & Giovinazzi, S. (2006). Macroseismic and mechanical models for the vulnerability and damage assessment of current buildings. *Bulletin of Earthquake Engineering*, 4(4), 415–443. doi:10.1007/s10518-006-9024-z

Lantada, N., Irizarry, J., Barbat, A. H., Goula, X., Roca, A., Susagna, T., & Pujades, L. G. (2010). Seismic hazard and risk scenarios for Barcelona, Spain, using the Risk-UE vulnerability index method. *Bulletin of Earthquake Engineering*, 8(2), 201–229. doi:10.1007/s10518-009-9148-z

Leca (2015). Sistemi e soluzioni tecniche per ristrutturare [Systems and technical solutions for renovation] in *Manuale Centro Storico*. Retrieved from https://www.leca.it/

Maio, R., Ferreira, T. M., Vicente, R., & Estêvão, J. (2016). Seismic vulnerability assessment of historical urban centres: Case study of the old city Centre of Faro, Portugal. *Journal of Risk Research*, 19(5), 551–580. doi:10.1080/13669877.2014.988285

Maio, R., Vicente, R., Formisano, A., & Varum, H. (2015). Seismic vulnerability of building aggregates through hybrid and indirect assessment techniques. *Bulletin of Earthquake Engineering*, 13(10), 2995–3014. doi:10.1007/s10518-015-9747-9

McGuire, R. K. (1995). Probabilistic seismic hazard analysis and design earthquakes: Closing the loop. *Bulletin of Seismological Society of America*, 85(5), 1275–1284.

National Group for Protection from earthquake GNDT (1993). Manuale per il rilevamento della vulnerabilità sismica degli edifici, istruzioni per la compilazione della scheda di 2° Livello [Manual for the detection of seismic vulnerability of buildings, instructions for completing the 2nd level form]. Retrieved from: http://emidius.mi.ingv.it/GNDT/.

National Institute of Geophysics and Vulcanology (n.d). Progetto DPC-INGV S1. Retrieved from: http://esse1-gis.mi.ingv.it/.

Peroni, A., & Tucci, G. (2010). *Nuove ricerche su Sant'Antimo*. Sant'Antimo: Alinea Editrice s.r.l.

Pierdicca, A., Clementi, F., Isidori, D., Concettoni, E., Cristalli, C., & Lenci, S. (2016). Numerical model upgrading of a historical masonry palace monitored with a wireless sensors network. *International Journal of Masonry Research and Innovation*, 1(1), 74–99. doi:10.1504/IJMRI.2016.074748

QGIS Development Team (2014). QGIS Geographic Information System. Open Source Geospatial Foundation Project. Retrieved from: http://qgis.osgeo.org.Qgisorg.doi:http://www.qgis.org/.

Quagliarini, E., Maracchini, G., & Clementi, F. (2017). Uses and limits of the Equivalent Frame Model on existing unreinforced masonry buildings for assessing their seismic risk: A review. *Journal of Building Engineering*, 10, 166–182. doi:10.1016/j.jobe.2017.03.004

Ruiz, M. F., Muttoni, A., & Kunz, J. (2010). Strengthening of flat slabs against punching shear using post-installed shear reinforcement. *ACI Structural Journal*, 107, 2–14.

Udías, A. (2003). Coburn and R. Spence – Earthquake Protection. *Journal of Seismology*, 7(4), 541. doi:10.1023/B:JOSE.0000005800.12265.8f

Uva, G., Sanjust, C. A., Casolo, S., & Mezzina, M. (2016). ANTAEUS project for the regional vulnerability assessment of the current building stock in historical centers. *International Journal of Architectural Heritage*, 10(1), 20–43. doi:10.1080/15583058.2014.935983

Vicente, R., Parodi, S., Lagomarsino, S., Varum, H., & Silva, J. A. R. M. (2011). Seismic vulnerability and risk assessment: Case study of the historic city Centre of Coimbra, Portugal. *Bulletin of Earthquake Engineering*, 9(4), 1067–1096. doi:10.1007/s10518-010-9233-3

Zuccaro, G., & Cacace, F. (2015). Seismic vulnerability assessment based on typological characteristics. The first level procedure "SAVE.". *Soil Dynamic and Earthquake Engineering*, 69, 262–269. doi:10.1016/j.soildyn.2014.11.003

Zuccaro, G., & Papa, F. (1997). Aggiornamento Delle Mappe a Scala Nazionale Di Vulnerabilità Sismica Delle Strutture Edilizie. Sintesi dei lavori condotti per il GNDT-SSN [Update of National Scale Maps of Seismic Vulnerability of Building Structures. Summary of the work carried out for the GNDT-SSN]. Retrived from: https://emidius.mi.ingv.it/GNDT2/Pubblicazioni/Bernardini/7.pdf.